Dominating recombination mechanisms in organic solar cells based on ZnPc and C_{60}

Wolfgang Tress,[1,2,a)] Karl Leo,[1] and Moritz Riede[1]
[1]*Institut für Angewandte Photophysik, Technische Universität Dresden, George-Bähr-Str. 1, 01069 Dresden, Germany*
[2]*Biomolecular and Organic Electronics, IFM, Linköping University, 58183 Linköping, Sweden*

(Received 7 March 2013; accepted 4 April 2013; published online 22 April 2013)

We investigate the dominating recombination mechanisms in bulk heterojunction solar cells, using a blend of ZnPc and C_{60} as model system. Analyzing the open-circuit voltage (V_{oc}) as a function of illumination intensity, we find that trap-assisted recombination dominates for low light intensities, whereas at 1 sun, direct/bimolecular recombination becomes important. The recombination parameters are not significantly influenced by the blend mixing ratio and are also valid for injected charges. By changing the hole transport layer, recombination at the contact is separately identified as further mechanism reducing V_{oc} at higher light intensities. © *2013 AIP Publishing LLC* [http://dx.doi.org/10.1063/1.4802276]

In the last few years, organic photovoltaics[1–5] has made enormous progress. Nevertheless, a significant further increase in efficiency is needed to fully leverage the large advantages of this technology. The active region of organic photovoltaics is usually a heterojunction with nanoscale morphology, making it challenging to obtain a microscopic understanding. This is particularly true for recombination, which is the most important intrinsic loss mechanism in solar cells. Recombination sets the equilibrium charge carrier density within the photoactive material by balancing the optical generation at open circuit: The lower the recombination, the higher the charge carrier density at a given illumination intensity and the higher the potential for a high open-circuit voltage V_{oc}.[6] The reason is that the electro-chemical potential, which is a representative energy of one charge carrier in an ensemble, increases with charge carrier density. This effect of recombination limiting the open-circuit voltage was experimentally shown for organic solar cells by charge carrier extraction and transient photovoltage decay experiments.[7,8]

When extracting charge carriers (e.g., at short circuit or the power-generating region of the current-voltage curve), recombination is in competition with the field-dependent extraction of charges and reduces the fill factor and eventually the short circuit current density J_{sc}, commonly used to determine the order of recombination. However, J_{sc} is not the most appropriate point of the current-voltage characteristics (J-V curve) to study recombination, as a considerable amount of charges is extracted. This was a matter of discussion in the last years[9,10] and focus was turned to V_{oc}.[11–14] Open circuit is much more suited to study recombination, especially if the contacts are selective, which means that all charge carriers are forced to recombine within the device at V_{oc}.[6]

Several studies on different polymer solar cells have identified geminate recombination,[15,16] bimolecular recombination,[16–20] trap-assisted recombination,[9,21–23] monomolecular recombination in general,[24] or even a combination of geminate and non-geminate recombination[25,26] as loss mechanisms. These results demonstrate the great controversy around this important topic.

In this contribution, we study the dependence of V_{oc} on light intensity examining a large intensity range (10 μW/cm^2–1 W/cm^2), which allows to clearly distinguish the order of the recombination (monomolecular/trap assisted and bimolecular/direct). Although discussed in literature,[12,14] trap-assisted recombination has not yet been identified as distinct recombination mechanism when examining V_{oc} as a function of light intensity. Commonly, only a superposition of direct and trap-assisted recombination was found as reason increasing the slope of V_{oc} as a function of the logarithm of the light intensity. However, due to their distinct dependencies on charge carrier density, a clear transition between the regions where one or the other mechanism dominates is expected, if these are really two separate mechanisms. Additionally, it is not clear where the huge amount of non-radiative recombination[27] results from and what role the contacts play. Here, we identify a transition between the two bulk recombination regimes. We separately visualize the influence of recombination at the electrode by using doped charge transport layers with tailored energy levels and work functions. The experimental data are modeled by drift-diffusion simulations including trap-assisted and direct recombination, and the energetics of the contact materials. We show that the results obtained from fitting J-V data under illumination hold for the (dark) injection current in forward direction as well. Consequently, we can quantify the contributions of the three recombination mechanisms as a function of light intensity.

The investigated solar cells are prepared by subsequent deposition of all layers in a vacuum chamber as described in Ref. 28. The stack of all devices reads: ITO/C_{60}:NDN1 (20 nm, 3 wt. %)/ZnPc:C_{60}(50 nm, *x*:*y*)/HTL(1 nm)/p-HTL (45 nm, 5 wt. %)/p-dopant(2 nm)/Al(100 nm). Here, HTL means hole transport layer, where Di-NPD (N,N-diphenyl-N,N-bis(4-(N,N-bis(naphth-1-yl)-amino)-biphenyl-4-yl)-benzidine, ionization potential (IP) of 5.3 eV) and MeO-TPD (N4, N4, N4′, N4′-tetrakis(4-methoxyphenyl)-[1,1′-biphenyl]-4,4′-diamine, IP = 5.1 eV) are applied. The p-dopant is NDP9 in

a)Electronic mail: woltr@ifm.liu.se

case of Di-NPD and NDP2 in case of MeO-TPD. NDN1 is an n-dopant. Details on the materials can be found in Ref. 28. Current-voltage characteristics are recorded under simulated sunlight (16 S-002 Solar Light Company Inc., Glennside USA). The intensity is measured by a calibrated silicon reference diode (Hamamatsu, S1337-33BQ) and adjusted by using neutral-density filters and by varying the distance between the specimen and the fiber coupled to the sun simulator.

Simulated *J-V* curves are obtained by drift-diffusion simulations[29] of the three-layer solar cell stack (n-C_{60}/blend/p-HTL) assuming a realistic doping concentration ($5 \times 10^{18}\,\mathrm{cm}^{-3}$) in the doped layers as boundary condition. Knowing the exact value is not required as the simulation results are independent of the doping concentration as long as the doped layers are highly conductive compared to the blend.[31] This is the case as a variation of the HTL thickness does not change the devices' series resistance.[28] Charge carrier mobilities are chosen to match the overall shape of the *J-V* curve (see Refs. 28 and 30), the dielectric constant is set to 4.9, which is close to impedance measurement data,[32] and the absorption profile is obtained from optical modeling (Details in Ref. 28). Regarding the discussion of V_{oc}, only the effective donor-acceptor gap $E_g^{DA} = \mathrm{IP}_{donor} - \mathrm{EA}_{acceptor}$ (EA is electron affinity), the effective densities of states, and the prevailing recombination mechanisms and their parameters are important. The strategy applied to find these parameters will be discussed later. Here, we review analytical approaches to V_{oc} as a function of light intensity in case of selective contacts and a spatially constant generation rate.

We start with the equation for V_{oc}, which directly results from the quasi-Fermi level splitting with the assumption of relaxed electron and hole states,[6,33]

$$eV_{oc} = E_g^{DA} - k_B T \ln \frac{N_C N_V}{np} \tag{1}$$

with n and p as electron and hole densities and N_C and N_V as effective densities of states. To adjust this classical semiconductor equation to disordered organic solids, additional parameters might be added, and the $N_{C/V}$ replaced.[34] If recombination happens via charge-transfer (CT) states and this process shall be treated separately from free charge carriers, E_g^{DA} might be identified with the energy of the CT state and an additional factor added to the argument of the logarithm.[6,35] However, the dependence of V_{oc} on $\ln(np)$ remains. Thus, the following statements are of general nature and valid for organic solar cells as well.

The expression np in Eq. (1) can be replaced by applying the approach of Ref. 6: Assuming selective contacts, the recombination rate R equals the generation rate G at V_{oc}. Thus, Eq. (1) can be rewritten for direct (bimolecular) recombination with $R_d = \beta np \stackrel{!}{=} G$,

$$\begin{aligned} eV_{oc} &= E_g^{DA} - k_B T \ln \frac{N_C N_V}{G/\beta} \\ &= E_g^{DA} - k_B T \ln \frac{N_C N_V \beta}{1\,\mathrm{m^3 s}} + k_B T \ln \frac{G}{1\,\mathrm{m^{-3} s^{-1}}}. \end{aligned} \tag{2}$$

This equation predicts that V_{oc} scales logarithmically with the illumination intensity because G is proportional to the incoming photon flux. The slope in a graph, where the illumination intensity is plotted in the logarithm to the base 10, is $k_B T/\log(\exp(1)) \approx 2.3 \times k_B T \approx 59\,\mathrm{mV/decade}$ ($T = 300\,\mathrm{K}$).

In case of indirect/trap-assisted recombination, R can be expressed by the Shockley-Read-Hall (SRH) theory, which gives in the simplest case $R_{SRH} \approx c_t N_t \frac{np}{n+p}$.[6,12,36] Here, c_t is the capture rate and N_t the concentration of traps. We combine both parameters in one coefficient $k_{SRH} = c_t N_t$. If the majority of the present charge carriers is photogenerated (i.e., $n_{ph} = p_{ph}$), this equation can be simplified to $R \approx k_{SRH} n_{ph}/2 = k_{SRH} p_{ph}/2$. Thus, $G \propto n_{ph}$. This proportionality is also valid close to the contacts, where a high background density (n_d, p_d) of one charge carrier species may exist due to low injection barriers, e.g., $n_d \gg n_{ph} = p_{ph} \gg p_d \rightarrow R \approx k_{SRH} p_{ph}$. Setting $R = G$ and replacing np in Eq. (1) yields in the SRH case,

$$\begin{aligned} eV_{oc} &= E_g^{DA} - k_B T \ln \frac{N_C N_V}{G^2 C} \\ &= E_g^{DA} - k_B T \ln \frac{N_C N_V C^{-1}}{1\,\mathrm{m^3 s}} + 2k_B T \ln \frac{G}{1\,\mathrm{m^{-3} s^{-1}}}. \end{aligned} \tag{3}$$

Here, C is a parameter containing k_{SRH}. The slope of V_{oc} plotted as a function of the common logarithm of G is $2.3 \times 2k_B T$. This value is twice the slope of V_{oc} for direct recombination. Therefore, the slope of V_{oc} as a function of the logarithm of the light intensity can be used to distinguish between both recombination mechanisms. This idea was discussed in a similar derivation for amorphous silicon devices in Ref. 37 and planar heterojunction organic solar cells in Ref. 38. It has also been applied several times when discussing recombination in organic solar cells.[12–14]

If contacts are not selective, $G = R$ does not hold at V_{oc} because charge carriers can be lost due to "surface/interface" recombination when diffusing to the "wrong" electrode. This competing process as well as a superposition of direct and SRH recombination are considered in the numerical simulation, also taking into account the correct charge carrier density profiles and the actual shape of G obtained from optical modeling.[28]

In Fig. 1(b), the open-circuit voltage is depicted as a function of the illumination intensity for devices comprising ZnPc:C_{60} blends with three different mixing ratios and the two different HTLs. We first discuss the case of Di-NPD as HTL (open symbols) providing with its lower lying HOMO a sufficiently large built-in potential to avoid recombination at the electrodes. The dashed-dotted lines are a guide to the eye indicating the slopes predicted by Eqs. (2) and (3). Compared to the experimental data, these lines visualize the transition from trap-assisted recombination towards direct recombination with intensity. For intensities larger than 1 sun, mainly direct recombination dominates whereas at intensities lower than a hundredth of a sun, SRH recombination completely governs V_{oc}. The transition from SRH to direct recombination with intensity is reasonable as the probability of direct recombination scales with n^2 and will superimpose SRH recombination even if all recombination parameters are fixed. In disordered materials, one might find additional reasons for this transition accompanied with the filling of a broad density of states. This results in the picture of free and trapped charges in a shift of the ratio between more mobile (free) and less mobile (trapped) charge carriers towards more free charges with intensity. If the dependence

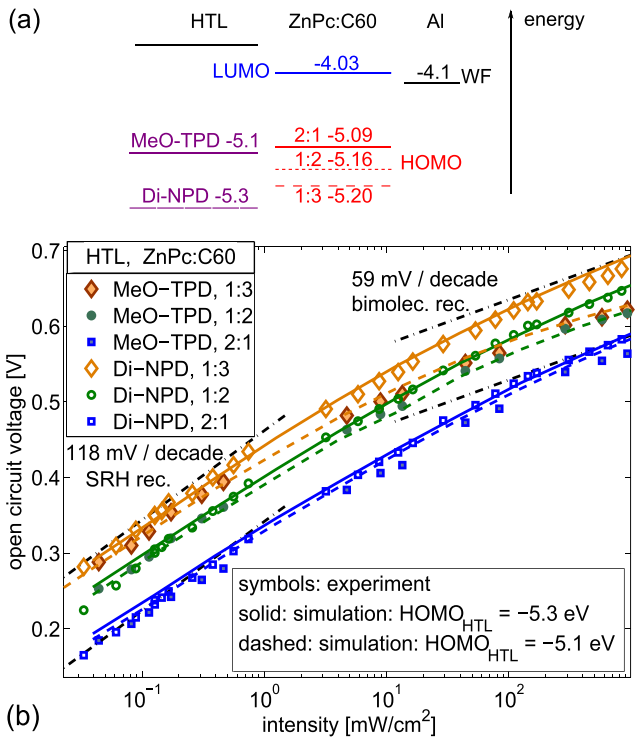

FIG. 1. (a) Energies, used in the simulation, for HOMO and LUMO of the ZnPc:C_{60} blends with different mixing ratios and the two different HTL MeO-TPD and Di-NPD. All values are given in eV and are based on experimentally determined values. (b) Open-circuit voltage as a function of illumination intensity measured with a calibrated reference diode. Roughly, $120 \pm 10\,\mathrm{mW\,cm^{-2}}$ represent 1 sun corrected for spectral mismatch, which slightly depends on the mixing ratio here given in volume percent. The dashed-dotted lines show the slopes expected from Eqs. (2) and (3). Symbols refer to experimental data and lines to simulation data, where a HOMO ($\approx -$ IP) of –5.1 eV represents MeO-TPD and −5.3 eV Di-NPD.

of V_{oc} on intensity shall be applied to identify the presence of trap-assisted recombination in a slope between 118 and 59 mV/decade, one should consider that this slope implies a region of transition between the two linear regimes (in a $V_{oc} - \ln(\text{intensity})$ plot) instead of fitting with a constant slope as commonly done.[13,14]

A variation of the mixing ratio results mainly in an offset of V_{oc}. The common shape of the curves in Fig. 1 indicates that the transition from SRH to direct recombination is not affected by the mixing ratio. Therefore, we conclude in a comparison with Eqs. (2) and (3) that either E_g^{DA} or $N_{C/V}$ change with mixing ratio whereas the recombination parameters β and k_{SRH} seem to be less influenced by the mixing ratio. Photoelectron spectroscopy measurements, characterizations of the energy of the CT-state,[32] and investigations on charge carrier extraction probabilities[39] indeed indicate a change of the IP and E_g^{DA} with mixing ratio. The reasons for this effect are most probably changes in the morphology of the blend including the growth modes of ZnPc.[32]

The closed symbols in Fig. 1(b) show data for almost identical devices except for the hole transport layer being interchanged with MeO-TPD, which has a lower IP (5.1 eV) than Di-NPD. Whereas the V_{oc} of the ZnPc:C_{60} 2:1 device is not affected, the V_{oc} values of the 1:2 and 1:3 blends with HTL MeO-TPD are reduced for higher light intensities. The reason is that due to the lower IP and subsequently lower work function of MeO-TPD, the built-in field in the device is reduced and an injection barrier from the HTL towards the ZnPc in the blend is formed. This means that for high open-circuit voltages close to the built-in potential, the electrical field as directive driving force vanishes and recombination of electrons at the MeO-TPD/blend interface sets in.[6,31] This effect is crucial for the blends with a higher content of C_{60} as the IP of these blends is larger [Fig. 1(a)].

A more quantitative analysis can be done with the aid of numerical simulations. Here, SRH recombination and direct recombination are each described by one parameter. They can be unambiguously determined from V_{oc} as a function of intensity if E_g^{DA} and $N_{C/V}$ are known. For setting E_g^{DA}, we choose the ionization potential of ZnPc considering the values measured at the blends with different stoichiometries by photoelectron spectroscopy[32] (variations of $\approx \pm 20$meV allowed). With a constant EA($\approx -$LUMO)[32] of C_{60} at 4.03 eV (from fit to the V_{oc} data, inverse photoemission spectroscopy gives a variety of data, e.g., 3.94 ± 0.1 eV (Ref. 40)), we fix E_g^{DA} and set $N_{C/V}$ to $10^{21}\mathrm{cm^{-3}}$, which is approximately the molecule density. This means we attribute, as already mentioned, the almost constant offset between the curves to a change in E_g^{DA} from 1.06 eV (ZnPc:C_{60} 2:1) to 1.13 eV (1:2) to 1.17 eV (1:3). Alternatively, significant changes of k_{SRH} (factor 10) and β (factor 100) with mixing ratio could sufficiently reproduce the data as well. This approach, however, requires a change of both parameters. In the picture of a diffusion-limited recombination for both trap-assisted and direct recombination, a correlation of both rate constants might be reasonable.[22] However, changed recombination parameters are supposed to be seen in transient photovoltage measurements.[7] As the decay times at a fixed intensity[30] are independent of mixing ratio, we conclude that the differences in V_{oc} are not attributed to changed recombination but a changed E_g^{DA}. Recombination kinetics independent of blend composition were also reported for polymer-based solar cells.[41]

The solid lines in Fig. 1(b) indicate that the intensity dependence can be reproduced with fixed values of $k_{SRH} = 10^6\mathrm{s^{-1}}$ and $\beta = 8 \times 10^{-12}\mathrm{cm^3 s^{-1}}$. Whereas V_{oc} is quite sensitive to k_{SRH}, the value of β has to be read as an order of magnitude rather than an exact number. Both values are in the range reported for organic solar cells.[12,42] The presence of deep electron traps in ZnPc:C_{60} blends was shown by impedance spectroscopy[43] with a concentration of $3 \times 10^{16}\mathrm{cm^{-3}}$. Assuming a characteristic reported[44] capture rate in the order of $10^{10}\mathrm{cm^3 s^{-1}}$ yields the value of k_{SRH} which we find. Langevin theory predicts a slightly (around 2 to 10 times) larger value for β than the one assumed here. Furthermore, the fixed β indicates that Langevin recombination is probably not applicable in these bulk heterojunction blends because the mobilities vary between different mixing ratios.[28] This non-applicability of Langevin theory to blends was often observed in literature and pre-factors were introduced.[42] Here, for a final statement, further investigations like transient charge extraction measurements are required. However, the changes in V_{oc} with mixing ratio cannot be explained by Langevin recombination. If we had assumed in the simulation that the gap was constant and changes in recombination had to explain the changes of V_{oc} between different mixing ratios, β would have to be decreased by two orders of magnitude for the 1:3 compared to the 2:1

blend. This change, however, does not follow the trends in mobilities, where the (higher) electron mobility increases roughly by a factor of five and the hole mobility decreases by a comparable extent when increasing the concentration of C_{60}.[28]

Only setting the IP of the HTL to 5.1 eV and not doing any fitting or changing any other parameter, results in simulation data represented by the dashed lines in Fig. 1(b), which reproduce the experimental data with MeO-TPD as HTL well.

We note that information about geminate recombination cannot be deduced in a study of V_{oc}. At V_{oc}, a possibly present geminate recombination is in dynamic equilibrium with free charge carriers via dissociation and formation of a bound electron/hole pair. The intensity dependence of V_{oc} will then follow the "recombination" process of free charge carriers into a bound pair (CT exciton). However, we were able to reproduce the complete shape of the *J-V* curve for different generation profiles without considering geminate recombination in competition with field-dependent dissociation of CT-states.[28] Therefore, we conclude that geminate recombination does not play a significant role in our material system.

The simulation allows to extract the amount of direct and SRH recombination as a function of light intensity and estimate the losses due to traps. Figure 2(a) shows the relation between radiative and SRH recombination for a 1:3 blend as a function of illumination intensity extracted from the simulation data assuming an IP of the HTL of 5.3 eV (Di-NPD). While the share of direct recombination increases from 5% to 70% with intensity, SRH recombination decreases from 95% to 30%. The differential slope $dV_{oc}/d\log(\text{Intensity})$ also shown in the figure (right axis) can be seen as a measure of the ratio between direct and SRH recombination. At short-circuit (dashed), the ratio between trap-assisted and direct recombination is slightly shifted towards SRH recombination at higher intensities due to lower charge carrier densities at short-circuit conditions compared to open circuit. This trend is inverted for lower light intensities as the charge carrier drift at short-circuit allows charge carriers to move a certain distance increasing the probability of a direct (bimolecular) encounter. Most of the charges are extracted at short circuit. Therefore, the overall recombination at short circuit compared to open circuit is reduced by around 70% to 80% depending on the light intensity. Figure 2(a) shows that even at 1 sun, there is a considerable contribution from SRH recombination (>50%). However, eliminating this process in simulation does not significantly increase V_{oc} (from 0.63 V to 0.64 V). Nevertheless, the efficiency increases from 2.4% to 2.9% due to a higher fill factor without SRH recombination. For intensities lower than 0.1 suns, however, V_{oc} and the efficiency are significantly limited by traps.

Figure 2(b) shows the share of the different recombination mechanisms for the low work function HTL MeO-TPD. In this case, as already discussed, recombination at the electrode can be identified at V_{oc} as a function of light intensity (Fig. 1). Hereby, it is critical to investigate a large intensity range to get unambiguous results. The share of recombination at the electrode (white area) increases with intensity and reaches more than 15%. It correlates well with the reduction of V_{oc} with HTL MeO-TPD compared to Di-NPD, which sets in at an intensity of 1 to 10 mW/cm^2 in Fig. 1(b). At short circuit (dashed), a significant recombination at the electrode cannot be observed, as charge carriers are driven towards the right electrode due to the electric field caused by the built-in potential.

The discussion so far focused on (separated) charge carriers which resulted from photogeneration. However, a self-consistent simulation is capable of describing the recombination of injected charges as well, as, e.g., demonstrated for bimolecular recombination in Ref. 45. To validate this, the forward current without illumination is investigated. A comparison of experimental with simulated data is shown in Fig. 3. The simulation data are obtained by using the parameters applied for the simulations discussed above and solely deactivating optical generation. Additionally, an experimentally detected shunt is considered, which dominates the *J-V* curves at current densities lower than

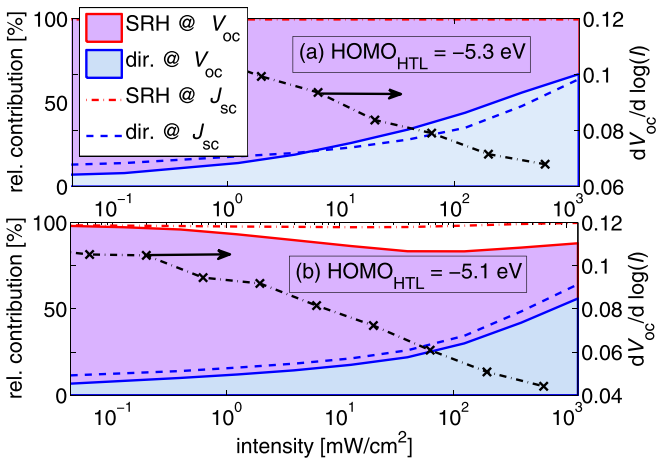

FIG. 2. Simulated share of trap-assisted (SRH) and direct/bimolecular recombination as a function of light intensity for the 1:3 blend at open circuit (colored areas surrounded by solid lines) and short-circuit (dashed). The share of direct recombination increases with light intensity, correlating with the differential slope (crosses) of the simulated V_{oc} as a function of light intensity from Fig. 1. For the higher lying HOMO of the HTL (b), a significant amount of recombination at the electrodes (white area) can be seen.

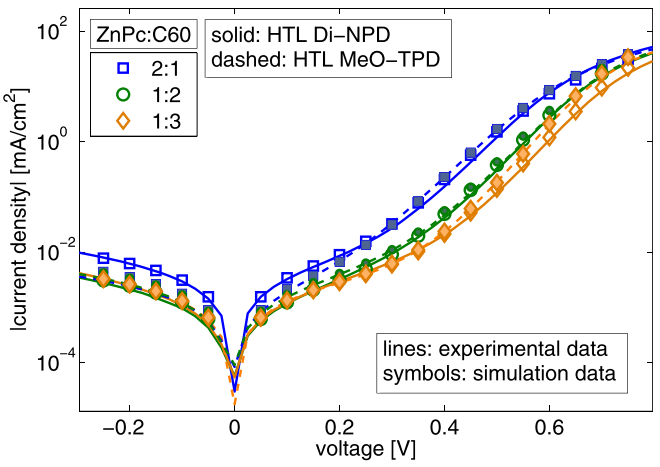

FIG. 3. Experimental (lines) and simulated (symbols) dark *J-V* curves for different mixing ratios. Solid lines represent devices with HTL Di-NPD and dashed lines devices with HTL MeO-TPD. Open symbols refer to a simulation with a HOMO of the HTL of −5.3 eV and closed symbols to a HOMO of −5.1 eV.

$0.01\,mA/cm^2$. Information on recombination is mainly found in the exponential region where the slope is dominated by recombination of injected electrons and holes. This slope corresponds to a diode ideality factor of around 1.9 and is very well reproduced by the simulations. Thus, the initial forward current at voltages up to ≈ 0.7 V is mainly dominated by SRH recombination, and the parameters obtained from V_{oc} describe also the dark forward current very well. However, these results show that the dominating recombination mechanism under 1 sun does not necessarily prevail in the exponential rise of the forward injection current, i.e., the diode ideality factor. For MeO-TPD, the current onset shifts to lower voltages as the built-in potential is lower in these devices. Especially in the case of the 1:3 blend, an increase of the slope in the exponential regime can be seen, which is reproduced by the simulation as well. This indicates that the recombination at the HTL/blend interface is direct/bimolecular, as assumed in the simulation.

All three recombination processes (direct, SRH, and at the interface to the p-HTL) are predominantly non-radiative and the share of radiative recombination measured by electroluminescence (wavelength <1100 nm) is in the order of $10^{-8} - 10^{-7}$ and reduced in case of MeO-TPD as HTL where most of the injection current is driven by electrons on C_{60} recombining at the HTL/blend interface.[30] This observation indicates that the radiative recombination is a bulk recombination process, where electron and hole meet and form an exciton which decays radiatively, although most of the direct electron-hole recombination is non-radiative.

In conclusion, we have identified the dominating recombination process in organic solar cell, using ZnPc:C_{60} as a model system. Recombination shifts from trap-assisted to direct/bimolecular recombination for higher intensities. This shift is independent of the bulk heterojunction mixing ratio and is seen in a change of the slope of V_{oc} as a function of light intensity. Introducing an injection barrier by changing the hole transport layer decreases V_{oc} for high light intensities due to a lower built-in field, which increases the probability for recombination at the HTL. All three recombination processes are predominantly non-radiative.

The authors want to thank the BMBF (OPEG, Grant No. 13N9720) for financial support. W.T. kindly acknowledges funding by the Reiner Lemoine foundation.

[1]G. Yu, J. Gao, J. C. Hummelen, F. Wudl, and A. J. Heeger, Science **270**, 1789 (1995).
[2]P. Peumans, S. Uchida, and S. R. Forrest, Nature **425**, 158 (2003).
[3]J. Y. Kim, K. Lee, N. E. Coates, D. Moses, T.-Q. Nguyen, M. Dante, and A. J. Heeger, Science (N.Y.) **317**, 222 (2007).
[4]G. Li, R. Zhu, and Y. Yang, Nat. Photonics **6**, 153 (2012).
[5]Y. Sun, G. C. Welch, W. L. Leong, C. J. Takacs, G. C. Bazan, and A. J. Heeger, Nature Mater. **11**, 44 (2012).
[6]W. Tress, K. Leo, and M. Riede, Phys. Rev. B **85**, 155201 (2012).
[7]A. Maurano, R. Hamilton, C. G. Shuttle, A. M. Ballantyne, J. Nelson, B. O'Regan, W. Zhang, I. McCulloch, H. Azimi, M. Morana, C. J. Brabec, and J. R. Durrant, Adv. Mater. **22**, 4987 (2010).
[8]D. Credgington, R. Hamilton, P. Atienzar, J. Nelson, and J. R. Durrant, Adv. Funct. Mater. **21**, 2744 (2011).
[9]R. A. Street and M. Schoendorf, Phys. Rev. B **81**, 205307 (2010).
[10]C. Deibel and A. Wagenpfahl, Phys. Rev. B **82**, 207301 (2010).
[11]L. J. A. Koster, V. D. Mihailetchi, R. Ramaker, and P. W. M. Blom, Appl. Phys. Lett. **86**, 123509 (2005).
[12]M. M. Mandoc, F. B. Kooistra, J. C. Hummelen, B. de Boer, and P. W. M. Blom, Appl. Phys. Lett. **91**, 263505 (2007).
[13]S. Cowan, A. Roy, and A. Heeger, Phys. Rev. B **82**, 245207 (2010).
[14]S. R. Cowan, W. L. Leong, N. Banerji, G. Dennler, and A. J. Heeger, Adv. Funct. Mater. **21**, 3083 (2011).
[15]S. De, T. Pascher, M. Maiti, K. G. Jespersen, T. Kesti, F. Zhang, O. Inganäs, A. Yartsev, and V. Sundström, J. Am. Chem. Soc. **129**, 8466 (2007).
[16]M. Mingebach, S. Walter, V. Dyakonov, and C. Deibel, Appl. Phys. Lett. **100**, 193302 (2012).
[17]C. Shuttle, B. O'Regan, A. Ballantyne, J. Nelson, D. Bradley, and J. Durrant, Phys. Rev. B **78**, 113201 (2008a).
[18]R. Mauer, I. A. Howard, and F. Laquai, J. Phys. Chem. Lett. **1**, 3500 (2010).
[19]J. Kniepert, M. Schubert, J. C. Blakesley, and D. Neher, J. Phys. Chem. Lett. **2**, 700 (2011).
[20]L. J. A. Koster, M. Kemerink, M. M. Wienk, K. Maturová, and R. A. J. Janssen, Adv. Mater. **23**, 1670 (2011).
[21]T. Kirchartz, B. Pieters, J. Kirkpatrick, U. Rau, and J. Nelson, Phys. Rev. B **83**, 115209 (2011).
[22]M. Kuik, L. Koster, G. Wetzelaer, and P. Blom, Phys. Rev. Lett. **107**, 256805 (2011).
[23]R. C. I. MacKenzie, C. G. Shuttle, M. L. Chabinyc, and J. Nelson, Adv. Energy Mater. **2**, 662 (2012).
[24]L. Liu and G. Li, Sol. Energy Mater. Sol. Cells **95**, 2557 (2011).
[25]D. Credgington, F. C. Jamieson, B. Walker, T.-Q. Nguyen, and J. R. Durrant, Adv. Mater. **24**, 2135 (2012).
[26]S. Albrecht, W. Schindler, J. Kurpiers, J. Kniepert, J. C. Blakesley, I. Dumsch, S. Allard, K. Fostiropoulos, U. Scherf, and D. Neher, J. Phys. Chem. Lett. **3**, 640 (2012).
[27]K. Vandewal, K. Tvingstedt, A. Gadisa, O. Inganäs, and J. V. Manca, Nature Mater. **8**, 904 (2009).
[28]W. Tress, M. Furno, M. Hein, and K. Leo, "Correlation of Absorption Profile and Fill Factor in Organic Solar Cells: The Role of Mobility Imbalance," Adv. Energy Mater. (published online).
[29]W. Tress, Ph.D. Dissertation, TU Dresden, 2011, available at http://nbn-resolving.de/urn:nbn:de:bsz:14-qucosa-89501.
[30]See supplementary material at http://dx.doi.org/10.1063/1.4802276 for simulation parameters, transient photovoltage, and electroluminescence measurements.
[31]W. Tress, K. Leo, and M. Riede, Adv. Funct. Mater. **21**, 2140 (2011).
[32]M. L. Tietze, W. Tress, S. Pfuetzner, C. Schuenemann, L. Burtone, M. Riede, K. Leo, K. Vandewal, S. Olthof, P. Schulz, and A. Kahn, "Correlation of the open-circuit voltage and the energy levels in zinc-phthalocyanine:C60 bulk heterojunction solar cells with varied mixing ratio" (unpublished).
[33]P. Würfel, *Physics of Solar Cells: From Basic Principles to Advanced Concepts* (Wiley-VCH, Weinheim, 2009).
[34]G. Garcia-Belmonte, Sol. Energy Mater. Sol. Cells **94**, 2166 (2010).
[35]K. Vandewal, K. Tvingstedt, A. Gadisa, O. Inganäs, and J. V. Manca, Phys. Rev. B **81**, 125204 (2010).
[36]W. Shockley and W. Read, Phys. Rev. **87**, 835 (1952).
[37]E. Schiff, Sol. Energy Mater. Sol. Cells **78**, 567 (2003).
[38]D. Cheyns, J. Poortmans, P. Heremans, C. Deibel, S. Verlaak, B. P. Rand, and J. Genoe, Phys. Rev. B **77**, 165332 (2008).
[39]W. Tress, S. Pfuetzner, K. Leo, and M. Riede, J. Photon. Energy **1**, 011114 (2011).
[40]A. Wilke, J. Endres, U. Hormann, J. Niederhausen, R. Schlesinger, J. Frisch, P. Amsalem, J. Wagner, M. Gruber, A. Opitz, A. Vollmer, W. Brutting, A. Kahn, and N. Koch, Appl. Phys. Lett. **101**, 233301 (2012).
[41]A. F. Nogueira, I. Montanari, J. Nelson, J. R. Durrant, C. Winder, N. S. Sariciftci, and C. Brabec, J. Phys. Chem. B **107**, 1567 (2003).
[42]A. Pivrikas, N. S. Sariciftci, G. Juška, and R. Österbacka, Prog. Photovoltaics **15**, 677 (2007).
[43]L. Burtone, D. Ray, K. Leo, and M. Riede, J. Appl. Phys. **111**, 064503 (2012).
[44]J. Bisquert, Phys. Rev. B **77**, 235203 (2008).
[45]C. G. Shuttle, A. Maurano, R. Hamilton, B. O'Regan, J. C. de Mello, and J. R. Durrant, Appl. Phys. Lett. **93**, 183501 (2008b).